Targeting USP22 with miR-30-5p to inhibit the hypoxia-induced expression of PD-L1 in lung adenocarcinoma cells

XIAOYANG HUA*, HENG CHU*, CHUANXIAO WANG, XUEXIN SHI, AILIN WANG and ZHE ZHANG

Department of Thoracic Surgery, Qingdao Municipal Hospital, Qingdao, Shandong 266000, P.R. China

Received November 15, 2020; Accepted May 21, 2021

DOI: 10.3892/or.2021.8166

Abstract. Lung cancer is one of the most common forms of cancer and accounts for a significant proportion of all cancer-related deaths. Lung adenocarcinoma (LUAD) accounts for approximately 40% of all cases of lung cancer. In recent years, new developments in both the diagnosis and treatment of LUAD have been achieved. Unfortunately, the prognosis remains poor for patients with malignant LUAD. Hypoxia is a common characteristic of solid tumors and induce the immune evasion by increasing the expression of programmed cell death-ligand-1 (PD-L1) in the tumor. In this study, it was predicted that ubiquitin-specific peptidase 22 (USP22) is the direct target of the microRNA (miR)-30-5p family, including miR-30a-5p, miR-30b-5p, miR-30c-5p, miR-30d-5p and miR-30e-5p. Furthermore, the binding of USP22 with the miR-30-5p family was confirmed by luciferase assay. In addition, it was demonstrated that targeting USP22 via the miR-30-5p family inhibited the induction of PD-L1 expression in hypoxic conditions, thus preventing activated T cells from killing LUAD cells. Our results indicated that miR-30a-5p, miR-30b-5p, miR-30c-5p, miR-30d-5p and miR-30e-5p represent new targets for the treatment of LUAD.

Introduction

Lung cancer is the most common form of cancer and represents a leading cause of cancer-related deaths worldwide (1). Lung adenocarcinoma (LUAD) accounts for approximately 40% of all cases involving lung cancer and is the most heterogeneous and aggressive form of non-small cell lung cancer (2,3). Despite new developments in the past few years in the diagnosis and treatment of LUAD, the prognosis of patients with malignant LUAD is poor; their 5-year survival rate, is <18% (4). Exploring the molecular mechanisms underlying the pathogenesis of LUAD and identifying new diagnostic biomarkers are essential to improve the prognosis of these patients.

The investigation of immune checkpoint inhibitors (ICIs) has led to significant changes in the therapeutic methods used in oncology, and in particular, the blockade of interactions involving programmed cell death-ligand 1 (PD-L1)/programmed cell death protein-1 (PD-1) (5). Tumor cells, by expressing PD-L1 and binding to PD-1 molecules on the surface of T cells, can activate negative co-stimulatory signals in T lymphocytes, thus inhibiting the activation and proliferation of T cells and the induction of apoptosis, thus allowing tumors to evade the surveillance of the immune system (6). The blockade of PD-L1/PD-1 has demonstrated favorable overall efficacies for the treatment of various types of tumor, and has been used clinically to treat non-small cell lung cancer (NSCLC) (7), melanoma (8), head and neck squamous cell carcinoma (HNSCC) (9,10), renal cell carcinoma (11), urothelial carcinoma (12), gastric cancer (13), microsatellite instability-high (MSI-H) cancers (14) and mismatch-repair deficiency (15). Because PD-L1 is expressed by tumor cells to inhibit T cells and survive their cytotoxic activities, the expression of PD-L1 in tumor tissue has been widely used as a favorable predictive biomarker for the diagnosis and prognosis of cancer (16,17). Hypoxia is the main feature of solid tumors. Studies have revealed that hypoxia can induce the expression of PD-L1 in tumor cells and facilitate the evasion of tumors from immune attack (18-20).

Ubiquitin-specific peptidase 22 (USP22) is a subunit of the human SPT-ADA-Gcn5 acetyltransferase (SAGA) complex and is a deubiquitinating enzyme (21). USP22 has been revealed to exhibit the transcriptional characteristics of different genes and can cause aggressive growth, metastasis, and treatment resistance, in numerous forms of human cancers, including lung cancer (22). A recent study revealed that USP22 could induce angiogenesis, growth and the metastasis of LUAD (23), thereby resulting in the development of LUAD. Study has also revealed that USP22 can stabilize PD-L1 protein expression in Human non-small cell lung cancer (24). However, whether USP22 can regulate the expression of PD-L1 in LUAD has yet to be elucidated.

Correspondence to: Dr Zhe Zhang, Department of Thoracic Surgery, Qingdao Municipal Hospital, 1 Jiaozhou Road, Qingdao, Shandong 266000, P.R. China
E-mail: zhang-elu@163.com

*Contributed equally

Key words: lung adenocarcinoma, microRNA-30-5p, ubiquitin-specific peptidase 22, programmed cell death-ligand 1, immune escape, hypoxia

Research has revealed that PD-1/PD-L1 plays a key role in the evasion of tumors from immune attack. Therefore, researchers have made numerous attempts to target this particular immune checkpoint (25). MicroRNAs (miRNAs or miRs) are short, non-coding, and evolutionarily conserved RNAs. miRNAs have been revealed to regulate gene expression at the post-transcription level by binding to the 3'-untranslated region (3'-UTR) of mRNAs (26). Multiple studies have reported that miRs can regulate PD-L1 expression via multiple pathways (27,28). Of these, miR-30-5p was reported to inhibit cell chemoresistance and stemness in colorectal cancer by targeting the USP22/Wnt/β-catenin signaling axis (29). Furthermore, miR-30-5p has also been revealed to function as a tumor suppressor in numerous different cancers (30). However, the relationship among miR-30-5p and USP22 and PD-L1 in LUAD cells has yet to be investigated.

Therefore, the aim of the present study was to investigate whether USP22 is the direct target of miR-30a-5p, miR-30b-5p, miR-30c-5p, miR-30d-5p and miR-30e-5p, and the relationship of inhibition of USP22 with the promotion of PD-L1 induced by hypoxia. It is theorized that the miR-30-5p family may represent a new treatment target for LUAD.

Materials and methods

Cell culture and transfection of oligomers. A549 cells, an important strain of LUAD cells were purchased from the Cell Bank of the Chinese Academy of Sciences (Shanghai, China). These cells were cultured in Roswell Park Memorial Institute (RPMI)-1640 medium (Sigma-Aldrich; Merck KGaA) with 10% fetal bovine serum (FBS) (Hyclone; Cytiva), 100 U/ml penicillin and 100 U/ml streptomycin at 37˚C. Incubation was carried out in a 5% CO_2 incubator with either 20% O_2 or 1% O_2. The 293T cell line was purchased from the American Type Culture Collection and cultured at 37˚C with 5% CO_2 in Dulbecco's modified Eagle's medium (DMEM) (Hyclone; Cytiva) supplemented with 10% FBS, 1% penicillin-streptomycin and 2 mM l-glutamine.

To perform miRNA mimics transfection, one day before transfection with miRNA mimics, 1x10^6 cells were seeded into 6-well plates and cultured at 37˚C with 5% CO_2. The transfection was performed when the cells had reached approximately 70% confluence using Lipofectamine RNAiMAX (Invitrogen; Thermo Fisher Scientific, Inc.) according to the manufacturer's instructions, and cells were cultured at 37˚C with 5% CO_2 for 48 h. Then, the level of miRNA was confirmed by RT-qPCR at 48 h post transfection. The miRNA oligonucleotides and control used in the study are listed in Table I. The final working concentration of the miRNA mimics was 100 nM. In addition, A549 cells were co-transfected with miR-30-5p mimics and a hypoxia response element (HRE) reporter gene plasmid (HRE-LUC). In addition, miR-30-5p mimics and Flag-USP22 or USP22 catalytic domain inactivated mutant plasmid (USP22-HH/AA), purchased from Shanghai GenePharma Co., Ltd, were co-transfected into A549 cells and cultured under hypoxic conditions. Lipofectamine 2000 (Invitrogen; Thermo Fisher Scientific, Inc.) was used for plasmid transfections following the manufacturer's instructions. For MG132 treatment, 5 mM stock solution was prepared by dissolving MG132 (Calbiochem; Merck KGaA) in DMSO. Then, the cells were treated with MG132 at a final concentration 25 μM for 24 h and collected for western blot assay.

Luciferase assay. The wild-type (WT) USP22 3'UTR or mutant (MUT) USP22 3'UTR containing the putative miR-30-5p binding site was synthesized (Sangon Biotech Co., Ltd.), and the fragments were cloned into the pMIR-Report Luciferase vector (Applied Biosystems; Thermo Fisher Scientific, Inc.). The 293T cell line was used for luciferase reporter assays. Cells were plated and the cell density was allowed to reach approximately 50%. Then, 100 ng pMIR/USP22 WT or pMIR/USP22 MUT, 2 ng *Renilla* luciferase plasmid (cat. no. E6921; Promega Corporation) containing *Renilla* luciferase and 100 nM miRNA mimics were co-transfected using Lipofectamine™ 2000 reagent. A total of 24 h after transfection, the firefly and *Renilla* luciferase activities were assessed using the Dual-Glo Luciferase Assay System (cat. no. E2920) and a GloMax® 20/20 Luminometer (E5311; both from Promega Corporation).

Reverse transcription-quantitative (RT-q) PCR. Total RNAs from A549 cells were extracted using RNAiso Plus (Takara Bio, Inc.). mRNAs were then reversely transcribed into complementary DNA with a reverse transcription kit (cat. no. RR036A; Takara Bio, Inc.) according to the manufacturer's instructions. The expression levels of mRNA and miRNA were then detected via TB Green II (cat. no. RR820Q; Takara Bio, Inc.). The thermocycling conditions were as follows: 94˚C for 4 min, followed by 35 cycles of 20 sec at 94˚C, 30 sec at 60˚C and 30 sec at 72˚C. β-actin and U6 were applied as internal controls. The relative expression levels were calculated with the $2^{-\Delta\Delta Cq}$ method (31). The primers are presented in Table II.

Western blot analysis. Cellular protein was extracted by RIPA Lysis Buffer (cat. no. P0013B; Beyotime Institute of Biotechnology) and protein concentrations were assessed with a BCA Protein Assay kit (cat. no. P0010; Beyotime Institute of Biotechnology) according to the manufacturer's instructions. A total of 30 μg protein was loaded per lane, and then the proteins were separated by 12% sodium dodecyl sulfate polyacrylamide gel electrophoresis (SDS-PAGE) and transferred to polyvinylidene fluoride (PVDF) membranes. Then membranes were blocked with 5% skim milk-TBST for 1 h at room temperature. Primary antibodies that were specific to PD-L1 (product no. 13684; 1:1,000; Cell Signaling Technology, Inc.), USP22 (cat. no. 55110-1-AP; 1:1,000; ProteinTech Group, Inc.), hypoxia-inducible factor (HIF)-1α (product no. 36169; 1:1,000; Cell Signaling Technology, Inc.), and β-actin (product no. 3700; 1:1,000; Cell Signaling Technology, Inc.), were incubated with the PVDF membranes for 12 h at 4˚C. PVDF membranes were incubated with HRP-conjugated goat anti-rabbit (cat. no. SA00001-2; 1:2,000) and goat anti-mouse (cat. no. SA00001-1; 1:2,000; ProteinTech Group, Inc.) IgG (H+L) secondary antibodies for 1 h at room temperature. Then, after being washed three times in PBS containing 0.05% Tween-20 (PBST), the membranes were visualized to demonstrate the positive binding antibody using BeyoECL Plus (cat. no. P0018S; Beyotime Institute of Biotechnology) and a gel imaging system (Bio-Rad Laboratories, Inc.). ImageJ v1.48 (National Institutes of Health) was then used to calculate the gray values of the images.

Table I. The sequences of transfected oligomers.

Name of miRNA	Sequences of transfected oligomers (5'-3')
miR-30a-5p	UGUAAACAUCCUCGACUGGAAGAAG
miR-30b-5p	UGUAAACAUCCUACACUCAGCU
miR-30c-5p	UGUAAACAUCCUACACUCUCAGC
miR-30d-5p	UGUAAACAUCCCCGACUGGAAG
miR-30e-5p	UGUAAACAUCCUUGACUGGAAG
miR-30e-5p control	UUCUCCGAACGUGUCACGUTT

miR, microRNA.

Table II. Primers for reverse transcription-quantitative PCR.

Gene name	Primer sequences
USP22	F: 5'-GGACAACTGGAAGCAGAACC-3'
	R: 5'-TGAAACAGCCGAAGAAGACA-3'
PD-L1	F: 5'-TAAGACCACCACCACCAA-3'
	R: 5'-TGACTATGATAGGCAGACATC-3'
β-actin	F: 5'-CACTGTGCCCATCTACGAGG-3'
	R: 5'-TAATGTCACGCACGATTTCC-3'
miR-30a-5p	F: 5'-ACACTCCAGCTGGGTGTAAACATC CTCGAC-3'
	R: 5'-CAGTGCGTGTCGTGGAGT-3'
miR-30b-5p	F: 5'-ACGGGCAAAAATACTCCAGCTCTC AAT-3'
	R: 5'-CTCTGGAAAACTGGTGTCGACTGG TGTC-3'
miR-30c-5p	F: 5'-GCCGCTGTAAACATC CTACACT-3'
	R: 5'-GTGCAGGGTCCGAGGT-3'
miR-30d-5p	F: 5'-GGTGTAAACATCCCCGAC-3'
	R: 5'-CAGTGCGTGTCGTGGAG-3'
miR-30e-5p	F: 5'-TGTAAACATCCTTGACTGGAAGG-3'
	R: 5'-CCAGTGCGAATACCTCGGAC-3'
U6	F: 5'-GCTTCGGCAGCACATATACT-3'
	R: 5'-GTGCAGGGTCCGAGGTATTC-3'

USP22, ubiquitin-specific peptidase 22; PD-L1, programmed cell death-ligand 1; miR, microRNA; F, forward; R, reverse.

T-cell-mediated tumor cell killing assay. According to an experiment previously reported (32), T cells were activated using anti-CD3 antibody (cat. no. 14-0037-82; 100 ng/ml; eBioscience; Thermo Fisher Scientific, Inc.) and interleukin-2 (cat. no. PHC0023; 10 ng/ml; Thermo Fisher Scientific, Inc.). After transfection with miRNA mimics, the cells were pre-treated at 37˚C under hypoxic conditions for 24 h, and the tumor cells and T cells were then co-cultured at 37˚C for 3 days. Next, the wells were washed twice with PBS to remove the T cells, and the surviving tumor cells were fixed with 4% paraformaldehyde for 20 min and stained with 1% crystal violet solution for 15 min at room temperature.

Cycloheximide (CHX) chase assay. Cells were treated with CHX (50 μg/ml; MedChemExpress) at 37˚C and harvested at 0, 4 and 8 h. After CHX treatment, cells were lysed in ice-cold RIPA cell lysates (CST) and the lysates were analyzed by western blotting with anti-HIF-1α, anti-USP22, anti-PD-L1 or anti-β-actin antibodies.

Co-immunoprecipitation (Co-IP). Cells were collected and immunoprecipitation was carried out with a Pierce™ Classic Magnetic IP/Co-IP kit (cat. no. 88804; Thermo Fisher Scientific, Inc.) in accordance with the manufacturer's instructions. Accordingly, cells were lysed in lysis buffer (0.025 M Tris, 0.15 M NaCl, 0.001 M EDTA, 1% NP-40, and 5% glycerin) for 5 min on ice, and then proteins were centrifugated at 13,000 x g for 10 min. Next, the samples were incubated with rabbit USP22 antibody (cat. no. 55110-1-AP; 4 μg; ProteinTech Group, Inc.) or rabbit isotype control IgG provided in the kit with agitated rotation at 4˚C overnight. Next, magnetic beads (0.25 mg) were added to the proteins and rotated at room temperature for 1 h. The magnetic beads were subsequently washed with buffer solution and eluted. Western blotting was then carried out as aforementioned.

Chromatin immunoprecipitation (ChIP) assay. Next, a Pierce Agarose ChIP kit (cat. no. 26156; Thermo Fisher Scientific, Inc.), and an HIF-1α or isotype control mAb (product no. 3900; Cell Signaling Technology, Inc.), were used for immunoprecipitation according to the manufacturer's instructions. Accordingly, the cultured cells were incubated with 1% formaldehyde for 10 min at 37˚C followed by incubation with 1X Glycine solution for 5 min at room temperature. Then, cells were collected, lysed, and digested by MNase. Next, protein-chromatin complexes were immunoprecipitated with 5 μg antibodies overnight at 4˚C with agitated rotation. Complexes were separated by incubation with ChIP grade proteinA/G agarose at 4˚C with agitation rotation for 1 h. Chromatin DNA fragments were then eluted and purified for quantitative real-time PCR. The products were then amplified using the following primers: HRE1 forward, 5'-TAC CATGCAGTAAGATGGGCAATA-3' and reverse, 5'-GAA CCCCAAAATGGAGTCCAAA-3'; HRE2 forward, 5'-GTA ATAGGAAGTATCAAAGTGCCC-3' and reverse, 5'-TCC CTCTTAGTGCCTCTCCAA-3'; HRE3 forward, 5'-TGCATA CAGTGGTTTTGGGA-3' and reverse, 5'-AGGAGTTCTACT TCCCTGAGT3'. anti-MYCN antibody (product no. 51705; Cell Signaling Technology, Inc.).

Statistical analysis. Results are expressed as the mean ± standard deviation (SD) of three independent experiments unless otherwise specified. Data were analyzed using Graph Prism version 8.2 software (GraphPad Software, Inc.). The unpaired Student's t-test and one-way analysis of variance (ANOVA) with Tukey's post hoc test were used to analyze differences between and among groups, respectively. $P<0.05$ was considered to indicate a statistically significant difference.

Results

miR-30-5p directly targets USP22. The miRNA targeted by USP22 was firstly predicted and a Venn diagram showing the

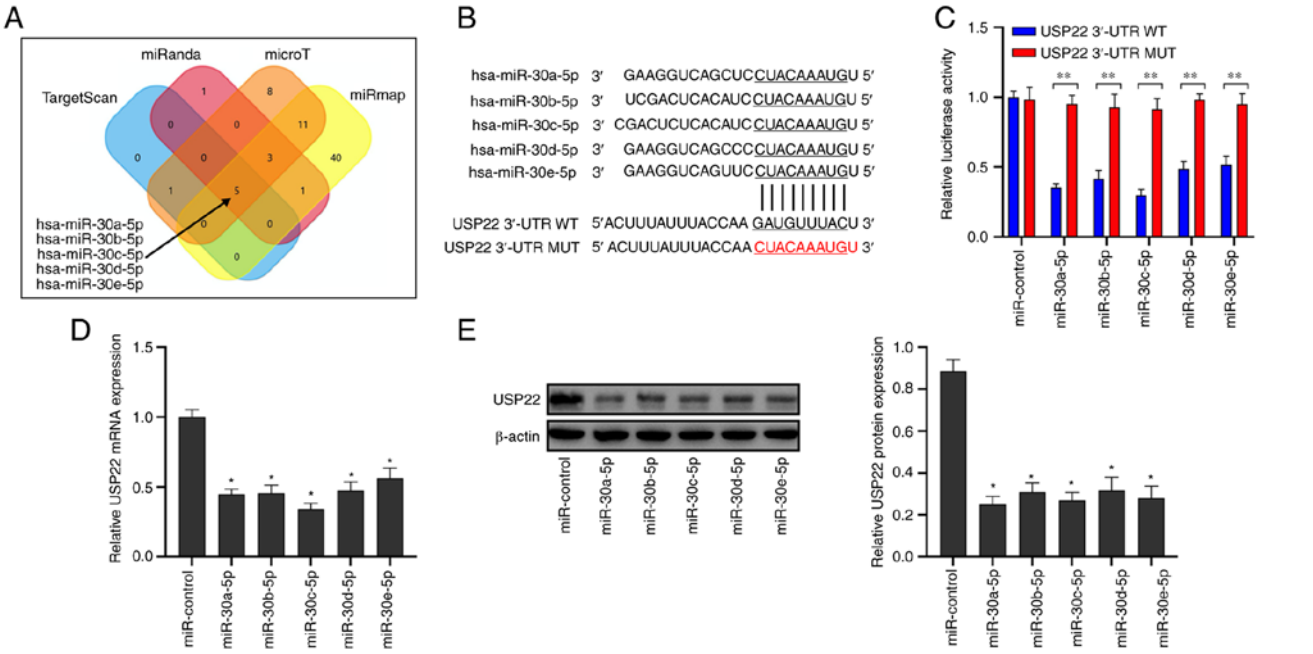

Figure 1. miR-30-5p directly targets USP22. (A) Overlapping sections of miRmap, microT, miRanda and TargetScan databases as shown by a Venn diagram. (B) The binding sites between the miR-30-5p family and the USP22 3'-UTR. (C) The luciferase activities of USP22 3'-UTR WT and USP22 3'-UTR MUT transfected with miR-30-5p or miR-control were determined by a dual-luciferase reporter assay. (D) The effects of miR-30-5p mimics on the expression of USP22 mRNA was analyzed through reverse transcription-quantitative PCR. (E) The effects of miR-30-5p mimics on the expression of USP22 protein was analyzed by western blotting. *P<0.05 compared with miR-control and **P<0.05. miR, microRNA; USP22, ubiquitin-specific peptidase 22; UTR, untranslated region; WT, wild-type; MUT, mutant.

overlapping parts of the four databases was generated (Fig. 1A). Analysis revealed that the miR-30-5p family targeted the 3'UTR bound to USP22 (Fig. 1B). The dual luciferase reporter results revealed that miR-30-5p significantly reduced the luciferase activity of wild-type USP22 3'-UTR, but did not affect the mutant USP22 3'-UTR (Fig. 1C; P<0.05). Transfection of miR-30-5p mimics significantly inhibited USP22 mRNA (Fig. 1D; P<0.05) and protein expression (Fig. 1E; P<0.05) in A549 cells. These results indicated that miR-30-5p directly targeted USP22 in A549 cells.

Expression of PD-L1 is inhibited in A549 cells under hypoxic conditions via the expression of miR-30-5p. Previous studies have reported that hypoxia induced the expression of PD-L1 and thus allows tumor cells to evade attack by the immune system (18-20). Firstly, miR-30a-5p mimics, miR-30b-5p mimics, miR-30c-5p mimics, miR-30d-5p mimics, miR-30e-5p mimics and the corresponding control were transfected in A549 cells. The transfection efficiency is revealed in Fig. S1. Next, it was investigated whether miR-30-5p could affect PD-L1 expression under hypoxic conditions (Fig. 2A; P<0.05). It was revealed that the transfection of miR-30-5p mimics inhibited the expression of PD-L1 mRNA (Fig. 2B; P<0.05) and protein (Fig. 2C; P<0.05) in A549 cells under hypoxic conditions; however, the overexpression of USP22 reversed this effect. These results indicated that miR-30-5p targeted USP22 to inhibit the expression of PD-L1 in A549 cells under hypoxic conditions.

Inducing the destruction of T cell-mediated A549 cells by targeting miR-30-5p via USP22 under hypoxia. Given that the binding of PD-L1 to PD-1 can inhibit T cell activation, and that miR-30-5p downregulated the expression of PD-L1 in A549 cells under hypoxia, it was next investigated whether miR-30-5p may have an effect on the mechanism by which A549 cells escape T cell-mediated cancer cell destruction. Our experiments demonstrated that incubating A549 cells with activated T cells could induce the death of T cells in A549 cells by the transfection of miR-30-5p mimics under hypoxic conditions; the overexpression of USP22 reversed this effect (Fig. 3). Therefore, this experiment indicated that targeting miR-30-5p via USP22 may induce LUAD cell destruction by T cell-mediation.

miR-30-5p inhibits HIF-1α binding to the HRE of the PD-L1 promoter region by down-regulating USP22 under hypoxia. It was revealed that miR-30-5p inhibits hypoxia-induced PD-L1 mRNA expression. A previous study reported that PD-L1 is the target gene of HIF-1α (19). It was hypothesized that the inhibition of hypoxia-induced PD-L1 mRNA expression by miR-30-5p may be related to HIF-1α. After co-transfected with miR-30-5p mimics and response element (HRE) reporter gene plasmid (HRE-LUC), the results showed that miR-30-5p mimics inhibited the luciferase activity of HRE-LUC (Fig. 4A; P<0.05). A previous study reported a potential HRE site on the PD-L1 gene (33) (Fig. 4B). Our chromatin immunoprecipitation results revealed that miR-30-5p inhibited the binding of HIF-1α to the PD-L1 gene HRE (Fig. 4C, P<0.05). These results indicated that miR-30-5p inhibited HIF-1α binding to the HRE of the PD-L1 promoter region under hypoxic conditions. To further verify whether miR-30-5p acts by targeting USP22, our experiments demonstrated that the co-transfection of USP22 and miR-30-5p mimics reversed the inhibitory effect of miR-30-5p mimics on the luciferase activity of

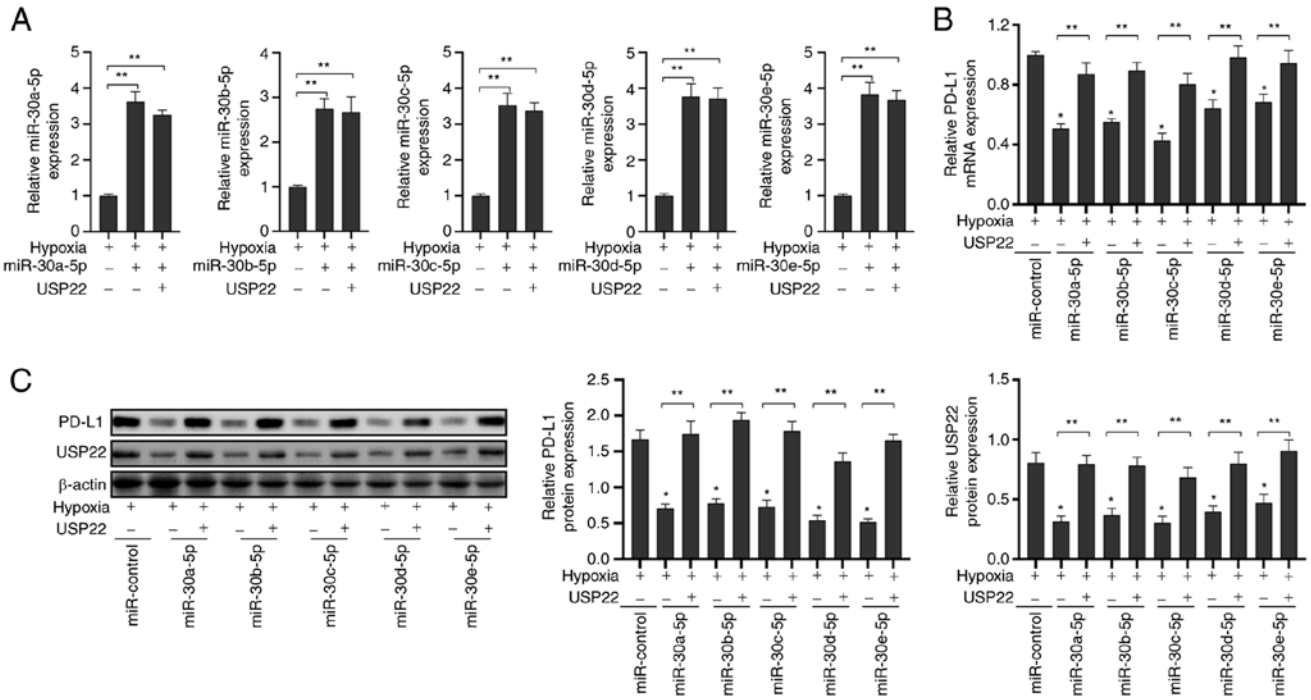

Figure 2. Expression of PD-L1 is inhibited in A459 cells under hypoxic conditions via the expression of miR-30-5p. (A) The effects of miR-30-5p mimics on the expression of miR-30-5p as determined by RT-qPCR. (B) The effects of miR-30-5p mimics on the expression of PD-L1 mRNA as determined by RT-qPCR. (C) The effects of miR-30-5p mimics on the expression of PD-L1 protein as determined by western blotting. *P<0.05 compared with miR-control and **P<0.05. PD-L1, programmed cell death-ligand 1; miR, microRNA; USP22, ubiquitin-specific peptidase 22; RT-qPCR, reverse transcription-quantitative PCR.

HRE-LUC (Fig. 4D; P<0.05), thus indicating that miR-30-5p inhibited HIF-1α binding to the HRE of the PD-L1 promoter region by targeting USP22 under hypoxia.

miR-30-5p inhibits the stabilizing effect on HIF-1α and PD-L1 protein by down-regulating USP22 under hypoxia. Next, it was analyzed whether miR-30-5p affected the stability of the PD-L1 and HIF-1α protein in A549 cells. Co-IP revealed that USP22 interacted with the PD-L1 and HIF-1α proteins in A549 cells under hypoxic conditions (Fig. 5A). Treatment with MG132, a proteasome inhibitor, reversed the inhibitory effect of miR-30-5p on PD-L1 and HIF-1α (Fig. 5B; P<0.05). Furthermore, miR-30-5p treatment shortened the half-life of both PD-L1 and HIF-1α (Fig. 5C). Our aforementioned results revealed that the co-transfection of miR-30-5p mimics and USP22 increased the expression of PD-L1 in A549 cells. Therefore, miR-30-5p mimics and Flag-USP22 or USP22 catalytic domain inactivated mutant plasmid (USP22-HH/AA) were co-transfected into A549 cells and cultured under hypoxic conditions. Compared with the co-transfection of miR-30-5p mimics and Flag-USP22 plasmids, the co-transfection of miR-30-5p mimics and USP22-HH/AA plasmid reduced the expression of PD-L1 and HIF-1α in A549 cells (Fig. 5D; P<0.05). These results indicated that miR-30-5p downregulated the expression of USP22 under hypoxic conditions, thus inhibiting its stabilizing effect on PD-L1 and HIF-1α protein, thereby inhibiting the expression of PD-L1 protein in A549 cells.

Discussion

The high mortality rate associated with LUAD is due to the lack of specific diagnostic biomarkers and effective

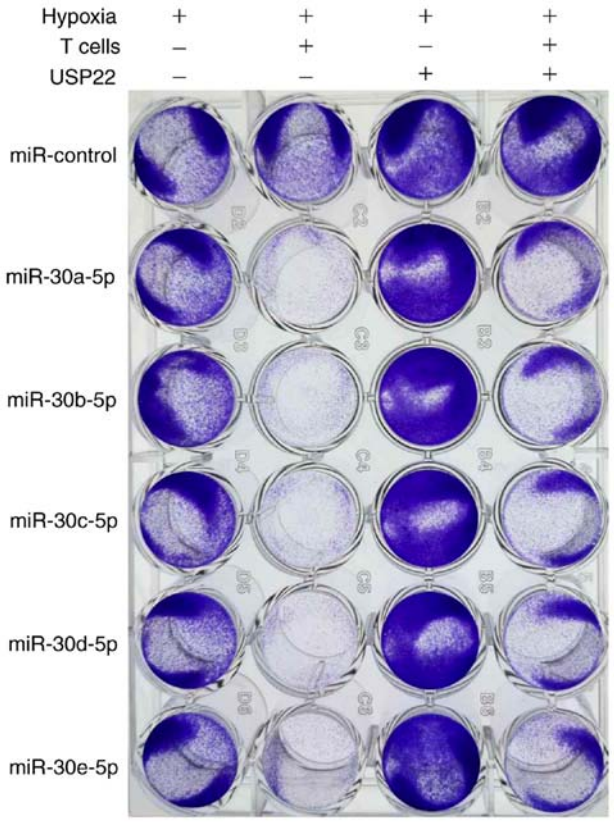

Figure 3. Inducing the destruction of T cell-mediated A549 by targeting miR-30-5p via USP22 under hypoxia. T cells were activated by a CD3 antibody (100 ng/ml) and interleukin-2 (10 ng/ml). After transfection with miRNA mimics, the cells were pre-treated under hypoxic conditions for 24 h and the tumor cells and T cells were co-cultured for 3 days. Staining was performed with crystal violet solution. miR, microRNA; USP22, ubiquitin-specific peptidase 22.

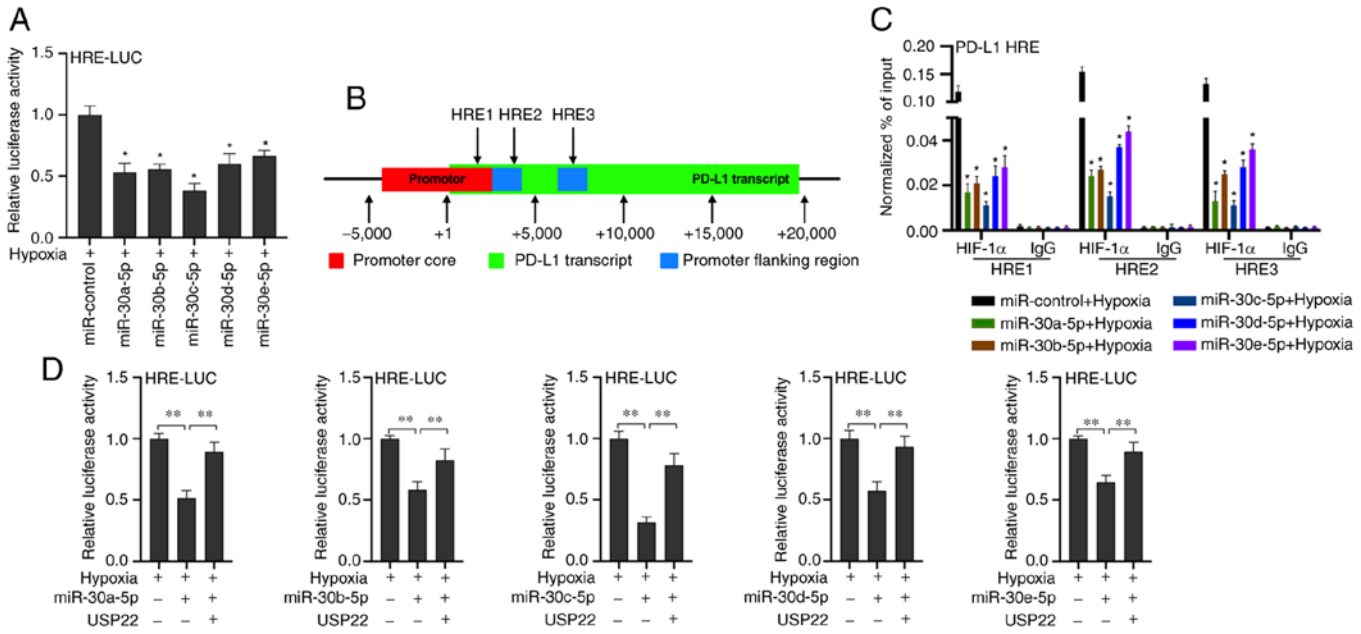

Figure 4. miR-30-5p inhibits HIF-1α binding to the HRE of the PD-L1 promoter region under hypoxia by targeting USP22. (A) The luciferase activities of the HRE transfected with miR-30-5p or miR-control as determined by a dual-luciferase reporter assay. (B) The potential HRE site of the PD-L1 gene. (C) The binding of HIF-1α to the PD-L1 gene HRE as determined by chromatin immunoprecipitation. (D) The luciferase activities of the HRE transfected with miR-30-5p or miR-control and a USP22 overexpression vector or empty vector as determined by a dual-luciferase reporter assay. *P<0.05 compared with miR-control and **P<0.05. miR, microRNA; HIF, hypoxia-inducible factor; HRE, hypoxia response element; PD-L1, programmed cell death-ligand 1; USP22, ubiquitin-specific peptidase 22.

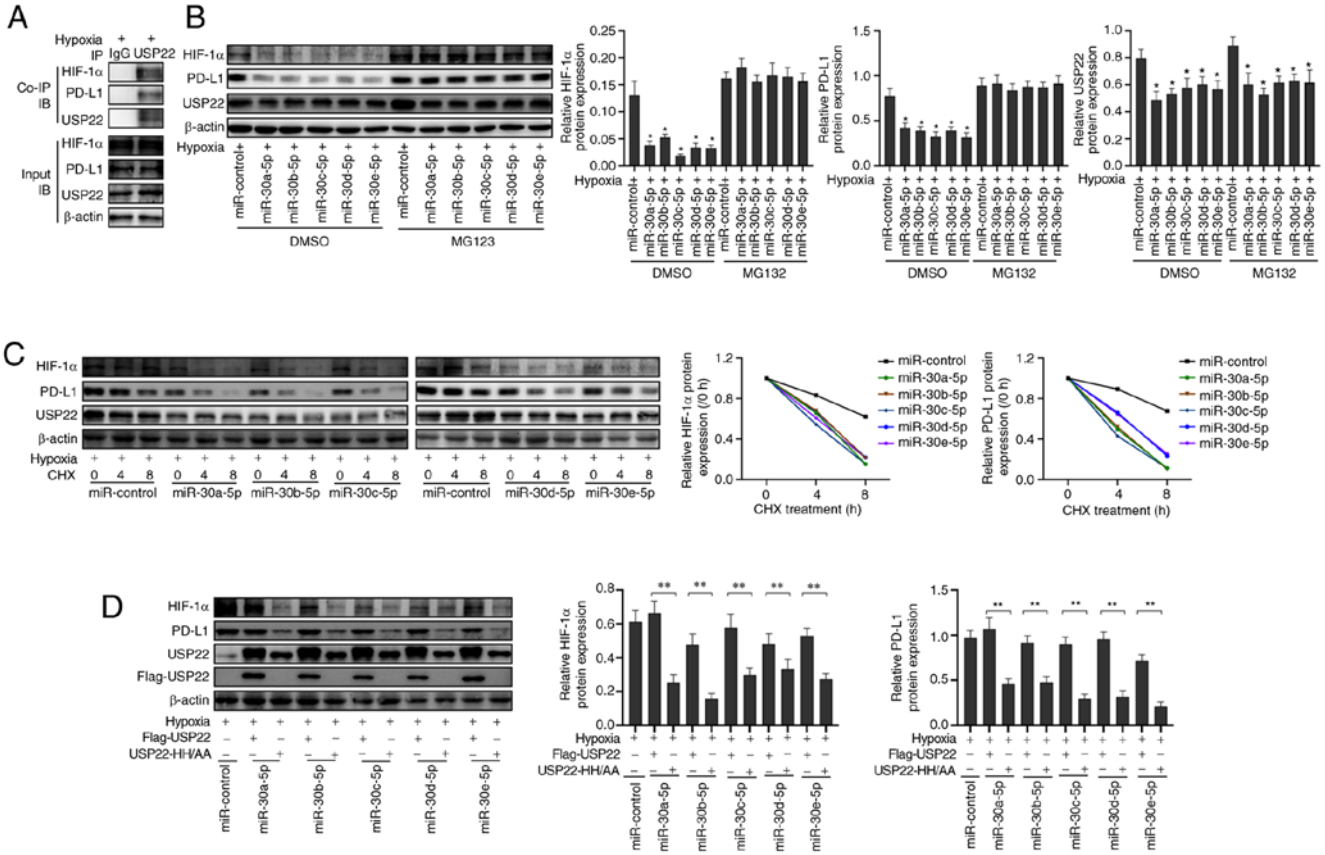

Figure 5. miR-30-5p inhibits the stabilizing effect on HIF-1α and PD-L1 protein by downregulating USP22 under hypoxia. (A) The interaction of USP22 protein with HIF-1α and PD-L1 proteins as determined by Co-IP. *P<0.05 compared with miR-control. (B) Western blot analysis of PD-L1 and HIF-1α protein expression in A549 cells transfected with the miR-30-5p family and treated with MG132. (C) Stability analysis of PD-L1 and HIF-1α proteins in A549 cells transfected with the miR-30-5p family and treated with CHX. *P<0.05 compared with miR-control. (D) Western blot analysis of PD-L1 and HIF-1α protein expression in A549 cells transfected with miR-30-5p mimics and Flag-USP22 or USP22 catalytic domain inactivated mutant plasmid (USP22-HH/AA). **P<0.05. miR, microRNA; HIF, hypoxia-inducible factor; PD-L1, programmed cell death-ligand 1; USP22, ubiquitin-specific peptidase 22; cycloheximide Co-IP, Co-immunoprecipitation.

therapeutic strategies. Understanding the novel mechanisms underlying the development of LUAD and identifying new targets to prevent the progression of LUAD represent key challenges in the improvement of LUAD treatment. MiRNAs are endogenous, non-coding, single-stranded, and small RNAs of 20-24 nucleotides in eukaryotes. MiRNAs play an important role in signal transduction, cell differentiation, proliferation, apoptosis, blood vessel formation and development, inflammation, and tumorigenesis, *in vivo* (34-36). The miR-30 family is an important member of the miRNA family. Mature miR-30 family members have a common seed sequence near the 5'-end, but have different compensation sequences near the 3'-end, allowing miR-30 family members to target different genes and pathways to perform corresponding biological functions (37). miR-30-5p has been revealed to function as a tumor suppressor in numerous different cancers (30). In particular, a previous study has demonstrated that the miR-30-5p family plays an important role in adenocarcinoma (38). For example, urinary miR-30a-5p was reported to be expressed at higher levels in stage I-II ovarian serous adenocarcinoma samples than that in stage III-IV samples, and also in well or moderately differentiated ovarian serous adenocarcinoma samples than in poorly differentiated samples (39). miR-30b-5p has been revealed to act as a tumor suppressor miRNA and to regulate cell proliferation and the cell cycle in esophageal squamous cell carcinoma (40). miR-30c-5p has been revealed to inhibit the aggressiveness of pancreatic ductal adenocarcinoma (PDAC) cells (38). Moreover, miR-30e-5p has been reported to reduce angiogenesis and metastasis targeting AEG-1 in head and neck squamous cell carcinoma (41). In colon cancer, miR-30-5p targeted the USP 22/Wnt/β-catenin signaling axis and thus increased chemo-sensitivity (29). Moreover, miR-30e-5p has been also reported to suppress non-small cell lung cancer tumorigenesis by regulating USP22-mediated Sirt1/JAK/STAT3 signaling (42). USP22 is a cytoplasmic and nuclear deubiquitinating enzyme that has been revealed to serve as an oncogene in a number of different types of cancer, including non-small cell lung cancer (42,43), papillary thyroid carcinoma (44) and glioma (45). Moreover, USP22 expression was revealed to be positively associated with PD-L1 expression in human non-small cell lung cancer samples (46). Furthermore, USP22 was revealed to upregulate MDMX, an murine double minute 2-related protein and inhibit p53 subsequently to promote NSCLC tumorigenesis (47). USP22 could also promote the proliferation of NSCLC cells via the stable expression of cyclooxygenase-2 (COX-2) (43). USP22 could also be targeted by miRNA-101 to inhibit the tumorigenesis of papillary thyroid carcinoma (44). However, the precise relationship between miR-30-5p and USP22 in LUAD has yet to be fully investigated. In the present study, it was revealed that the miR-30 family directly targeted USP22 in LUAD, thus indicating that miR-30-5p could regulate the progression of LUAD by targeting USP22.

Study has revealed that the expression of PD-L1 is closely related to tumor grade in several types of malignant tumors, and has become a new biomarker for tumor diagnosis and prognosis (48). PD-L1 is highly expressed in tumor cells and binds to TCR PD-1 leading to the negative regulation of T cell responses. This leads to tumor antigen-specific T cell-induced apoptosis, thus allowing cancer cells to evade immune surveillance and cell death (16,49-51). Hypoxia is the main feature of solid tumors. Studies have reported that hypoxia can induce tumor cells to express PD-L1 (18-20). In the present study, it was demonstrated that USP22 could stabilize hypoxia-induced PD-L1 expression in LUAD cells, thus indicating that USP22 plays a key role in the immune evasion of LUAD.

In the present study, the role of USP22 in the immune evasion of LUAD was examined. It was revealed that the miR-30-5p family inhibited the expression of PD-L1 in A549 cells by targeting USP22 under hypoxic conditions, thereby enhancing the destruction of A549 cells by activated T cells. Furthermore, miR-30-5p family regulated PD-L1 expression through USP22 at the level of transcription and by post-translational modification. Targeting USP22 with the miR-30-5p family directly inhibited its stabilizing effect on PD-L1 protein and regulated the expression of PD-L1 at the post-translational modification level. The miR-30-5p family also inhibited its stabilizing effect on HIF-1α protein, thereby inhibiting the transcription of its target gene PD-L1 by regulating USP22. In addition, the miR-30-5p family regulated the expression of PD-L1 at the transcription level. These findings indicated that the miR-30-5p family could inhibit the hypoxia-induced expression of PD-L1 in LUAD cells, which may serve as a target for inhibiting the hypoxia-induced immune evasion of LUAD cells.

Collectively, our experiments demonstrated that the miR-30 family plays an important role in the hypoxic-induced immune evasion of LUAD by targeting USP22. Consequently, USP22 may serve as an inhibitor of LUAD immune escape. Thus, our present findings provided new options for the treatment of lung adenocarcinoma.

Acknowledgments

Not applicable.

Funding

The present study was supported by the Qingdao Municipal Commission of Health and Family Planning (grant no. DTR2017Y18).

Availability of data and materials

The datasets used and/or analyzed during the current study are available from the corresponding author on reasonable request.

Authors' contributions

XH designed the study and wrote the manuscript. XH, HC and CW performed the experiments. XS and AW were in charge of confirming the authenticity of the raw data and data analysis. ZZ was the project leader, responsible for the design of the project and the revision of the manuscript. All authors read and approved the final manuscript.

Ethics approval and consent to participate

Not applicable.

Patient consent for publication

Not applicable.

Competing interests

The authors declare that they have no competing interests.

References

1. Bray F, Ferlay J, Soerjomataram I, Siegel RL, Torre LA and Jemal A: Global cancer statistics 2018: GLOBOCAN estimates of incidence and mortality worldwide for 36 cancers in 185 countries. CA Cancer J Clin 68: 394-424, 2018.
2. Travis WD, Brambilla E, Noguchi M, Nicholson AG, Geisinger KR, Yatabe Y, Beer DG, Powell CA, Riely GJ, Van Schil PE, *et al*: International association for the study of lung cancer/american thoracic society/european respiratory society international multidisciplinary classification of lung adenocarcinoma. J Thorac Oncol 6: 244-285, 2011.
3. Senosain MF and Massion PP: Intratumor heterogeneity in early lung adenocarcinoma. Front Oncol 10: 349, 2020.
4. Hirsch FR, Scagliotti GV, Mulshine JL, Kwon R, Curran WJ Jr, Wu YL and Paz-Ares L: Lung cancer: Current therapies and new targeted treatments. Lancet 389: 299-311, 2017.
5. Dong H, Strome SE, Salomao DR, Tamura H, Hirano F, Flies DB, Roche PC, Lu J, Zhu G, Tamada K, *et al*: Tumor-associated B7-H1 promotes T-cell apoptosis: A potential mechanism of immune evasion. Nat Med 8: 793-800, 2002.
6. Kim JM and Chen DS: Immune escape to PD-L1/PD-1 blockade: Seven steps to success (or failure). Ann Oncol 27: 1492-1504, 2016.
7. Herbst RS, Baas P, Kim DW, Felip E, Pérez-Gracia JL, Han JY, Molina J, Kim JH, Arvis CD, Ahn MJ, *et al*: Pembrolizumab versus docetaxel for previously treated, PD-L1-positive, advanced non-small-cell lung cancer (KEYNOTE-010): A randomised controlled trial. Lancet 387: 1540-1550, 2016.
8. Goldberg SB, Gettinger SN, Mahajan A, Chiang AC, Herbst RS, Sznol M, Tsiouris AJ, Cohen J, Vortmeyer A, Jilaveanu L, *et al*: Pembrolizumab for patients with melanoma or non-small-cell lung cancer and untreated brain metastases: Early analysis of a non-randomised, open-label, phase 2 trial. Lancet Oncol 17: 976-983, 2016.
9. Cohen EEW, Soulières D, Le Tourneau C, Dinis J, Licitra L, Ahn MJ, Soria A, Machiels JP, Mach N, Mehra R, *et al*: Pembrolizumab versus methotrexate, docetaxel, or cetuximab for recurrent or metastatic head-and-neck squamous cell carcinoma (KEYNOTE-040): A randomised, open-label, phase 3 study. Lancet 393: 156-167, 2019.
10. Bauml J, Seiwert TY, Pfister DG, Worden F, Liu SV, Gilbert J, Saba NF, Weiss J, Wirth L, Sukari A, *et al*: Pembrolizumab for platinum-and cetuximab-refractory head and neck cancer: Results from a single-arm, phase II study. J Clin Oncol 35: 1542-1549, 2017.
11. Motzer RJ, Escudier B, McDermott DF, George S, Hammers HJ, Srinivas S, Tykodi SS, Sosman JA, Procopio G, Plimack ER, *et al*: Nivolumab versus everolimus in advanced renal-cell carcinoma. N Engl J Med 373: 1803-1813, 2015.
12. Powles T, Durán I, van der Heijden MS, Loriot Y, Vogelzang NJ, De Giorgi U, Oudard S, Retz MM, Castellano D, Bamias A, *et al*: Atezolizumab versus chemotherapy in patients with platinum-treated locally advanced or metastatic urothelial carcinoma (IMvigor211): A multicentre, open-label, phase 3 randomised controlled trial. Lancet 391: 748-757, 2018.
13. Kang YK, Boku N, Satoh T, Ryu MH, Chao Y, Kato K, Chung HC, Chen JS, Muro K, Kang WK, *et al*: Nivolumab in patients with advanced gastric or gastro-oesophageal junction cancer refractory to, or intolerant of, at least two previous chemotherapy regimens (ONO-4538-12, ATTRACTION-2): A randomised, double-blind, placebo-controlled, phase 3 trial. Lancet 390: 2461-2471, 2017.
14. Overman MJ, Lonardi S, Wong KY, Lenz HJ, Gelsomino F, Aglietta M, Morse MA, Van Cutsem E, McDermott R, Hill A, *et al*: Durable clinical benefit with nivolumab plus ipilimumab in DNA mismatch repair-deficient/microsatellite instability-high metastatic colorectal cancer. J Clin Oncol 36: 773-779, 2018.
15. Le DT, Durham JN, Smith KN, Wang H, Bartlett BR, Aulakh LK, Lu S, Kemberling H, Wilt C, Luber BS, *et al*: Mismatch repair deficiency predicts response of solid tumors to PD-1 blockade. Science 357: 409-413, 2017.
16. Velcheti V, Schalper KA, Carvajal DE, Anagnostou VK, Syrigos KN, Sznol M, Herbst RS, Gettinger SN, Chen L and Rimm DL: Programmed death ligand-1 expression in non-small cell lung cancer. Lab Invest 94: 107-116, 2014.
17. Hamanishi J, Mandai M, Iwasaki M, Okazaki T, Tanaka Y, Yamaguchi K, Higuchi T, Yagi H, Takakura K, Minato N, *et al*: Programmed cell death 1 ligand 1 and tumor-infiltrating CD8+ T lymphocytes are prognostic factors of human ovarian cancer. Proc Natl Acad Sci USA 104: 3360-3365, 2007.
18. Vito A, El-Sayes N and Mossman K: Hypoxia-driven immune escape in the tumor microenvironment. Cells 9: 992, 2020.
19. Jiang X, Wang J, Deng X, Xiong F, Ge J, Xiang B, Wu X, Ma J, Zhou M, Li X, *et al*: Role of the tumor microenvironment in PD-L1/PD-1-mediated tumor immune escape. Mol Cancer 18: 10, 2019.
20. You L, Wu W, Wang X, Fang L, Adam V, Nepovimova E, Wu Q and Kuca K: The role of hypoxia-inducible factor 1 in tumor immune evasion. Med Res Rev 41: 1622-1643, 2021.
21. Pfoh R, Lacdao IK and Saridakis V: Deubiquitinases and the new therapeutic opportunities offered to cancer. Endocr Relat Cancer 22: T35-T54, 2015.
22. Melo-Cardenas J, Zhang Y, Zhang DD and Fang D: Ubiquitin-specific peptidase 22 functions and its involvement in disease. Oncotarget 7: 44848-44856, 2016.
23. Zhang K, Yang L, Wang J, Sun T, Guo Y, Nelson R, Tong TR, Pangeni R, Salgia R and Raz DJ: Ubiquitin-specific protease 22 is critical to in vivo angiogenesis, growth and metastasis of non-small cell lung cancer. Cell Commun Signal 17: 167, 2019.
24. Huang X, Zhang Q, Lou Y, Wang J, Zhao X, Wang L, Zhang X, Li S, Zhao Y, Chen Q, *et al*: USP22 Deubiquitinates CD274 to suppress anticancer immunity. Cancer Immunol Res 7: 1580-1590, 2019.
25. Sunshine J and Taube JM: PD-1/PD-L1 inhibitors. Curr Opin Pharmacol 23: 32-38, 2015.
26. Santos RM, Moreno C and Zhang WC: Non-Coding RNAs in lung tumor initiation and progression. Int J Mol Sci 21: 2774, 2020.
27. Chen J, Jiang CC, Jin L and Zhang XD: Regulation of PD-L1: A novel role of pro-survival signalling in cancer. Ann Oncol 27: 409-416, 2016.
28. Dong P, Xiong Y, Yu J, Chen L, Tao T, Yi S, Hanley SJ, Yue J, Watari H and Sakuragi N: Control of PD-L1 expression by miR-140/142/340/383 and oncogenic activation of the OCT4-miR-18a pathway in cervical cancer. Oncogene 37: 5257-5268, 2018.
29. Jiang S, Miao D, Wang M, Lv J, Wang Y and Tong J: miR-30-5p suppresses cell chemoresistance and stemness in colorectal cancer through USP 22/Wnt/β-catenin signaling axis. J Cell Mol Med 23: 630-640, 2019.
30. Zhao JJ, Lin J, Zhu D, Wang X, Brooks D, Chen M, Chu ZB, Takada K, Ciccarelli B, Admin S, *et al*: miR-30-5p functions as a tumor suppressor and novel therapeutic tool by targeting the oncogenic Wnt/β-catenin/BCL9 pathway. Cancer Res 74: 1801-1813, 2014.
31. Schmittgen TD and Livak KJ: Analyzing real-time PCR data by the comparative C(T) method. Nat Protoc 3: 1101-1108, 2008.
32. Sun X, Li CW, Wang WJ, Chen MK, Li H, Lai YJ, Hsu JL, Koller PB, Chan LC, Lee PC, *et al*: Inhibition of c-MET upregulates PD-L1 expression in lung adenocarcinoma. Am J Cancer Res 10: 564-571, 2020.
33. Avendaño-Ortiz J, Maroun-Eid C, Martín-Quirós A, Toledano V, Cubillos-Zapata C, Gómez-Campelo P, Varela-Serrano A, Casas-Martin J, Llanos-González E, Alvarez E, *et al*: PD-L1 overexpression during endotoxin tolerance impairs the adaptive immune response in septic patients via HIF1α. J Infect Dis 217: 393-404, 2018.
34. Lin YH: MicroRNA networks modulate oxidative stress in cancer. Int J Mol Sci 20: 4497, 2019.
35. Chandan K, Gupta M and Sarwat M: Role of host and pathogen-derived microRNAs in immune regulation during infectious and inflammatory diseases. Front Immunol 10: 3081, 2020.
36. Zhao Z, Sun W, Guo Z, Zhang J, Yu H and Liu B: Mechanisms of lncRNA/microRNA interactions in angiogenesis. Life Sci 254: 116900, 2020.
37. Mao L, Liu S, Hu L, Jia L, Wang H, Guo M, Chen C, Liu Y and Xu L: miR-30 family: A promising regulator in development and disease. Biomed Res Int 2018: 9623412, 2018.

38. Tanaka T, Okada R, Hozaka Y, Wada M, Moriya S, Satake S, Idichi T, Kurahara H, Ohtsuka T and Seki N: Molecular pathogenesis of pancreatic ductal adenocarcinoma: Impact of miR-30c-5p and miR-30c-2-3p regulation on oncogenic genes. Cancers (Basel) 12: 2731, 2020.
39. Zhou J, Gong G, Tan H, Dai F, Zhu X, Chen Y, Wang J, Liu Y, Chen P, Wu X and Wen J: Urinary microRNA-30a-5p is a potential biomarker for ovarian serous adenocarcinoma. Oncol Rep 33: 2915-2923, 2015.
40. Xu J, Lv H, Zhang B, Xu F, Zhu H, Chen B, Zhu C and Shen J: miR-30b-5p acts as a tumor suppressor microRNA in esophageal squamous cell carcinoma. J Thorac Dis 11: 3015-3029, 2019.
41. Zhang S, Li G, Liu C, Lu S, Jing Q, Chen X, Zheng H, Ma H, Zhang D, Ren S, *et al*: miR-30e-5p represses angiogenesis and metastasis by directly targeting AEG-1 in squamous cell carcinoma of the head and neck. Cancer Sci 111: 356-368, 2020.
42. Xu G, Cai J, Wang L, Jiang L, Huang J, Hu R and Ding F: MicroRNA-30e-5p suppresses non-small cell lung cancer tumorigenesis by regulating USP22-mediated Sirt1/JAK/STAT3 signaling. Exp Cell Res 362: 268-278, 2018.
43. Xiao H, Tian Y, Yang Y, Hu F, Xie X, Mei J and Ding F: USP22 acts as an oncogene by regulating the stability of cyclooxygenase-2 in non-small cell lung cancer. Biochem Biophys Res Commun 460: 703-708, 2015.
44. Zhao H, Tang H, Huang Q, Qiu B, Liu X, Fan D, Gong L, Guo H, Chen C, Lei S, *et al*: miR-101 targets USP22 to inhibit the tumorigenesis of papillary thyroid carcinoma. Am J Cancer Res 6: 2575-2586, 2016.
45. Li ZH, Yu Y, DU C, Fu H, Wang J and Tian Y: RNA interference-mediated USP22 gene silencing promotes human brain glioma apoptosis and induces cell cycle arrest. Oncol Lett 5: 1290-1294, 2013.
46. Wang Y, Sun Q, Mu N, Sun X, Wang Y, Fan S, Su L and Liu X: The deubiquitinase USP22 regulates PD-L1 degradation in human cancer cells. Cell Commun Signal 18: 112, 2020.
47. Ding F, Bao C, Tian Y, Xiao H, Wang M, Xie X, Hu F and Mei J: USP22 promotes NSCLC tumorigenesis via MDMX up-regulation and subsequent p53 inhibition. Int J Mol Sci 16: 307-320, 2014.
48. Mischinger J, Comperat E, Schwentner C, Stenzl A and Gakis G: Inflammation and cancer: What can we therapeutically expect from checkpoint inhibitors? Curr Urol Rep 16: 59, 2015.
49. Thompson RH, Gillett MD, Cheville JC, Lohse CM, Dong H, Webster WS, Krejci KG, Lobo JR, Sengupta S, Chen L, *et al*: Costimulatory B7-H1 in renal cell carcinoma patients: Indicator of tumor aggressiveness and potential therapeutic target. Proc Natl Acad Sci USA 101: 17174-17179, 2004.
50. Boland JM, Kwon ED, Harrington SM, Wampfler JA, Tang H, Yang P and Aubry MC: Tumor B7-H1 and B7-H3 expression in squamous cell carcinoma of the lung. Clin Lung Cancer 14: 157-163, 2013.
51. Cooper WA, Tran T, Vilain RE, Madore J, Selinger CI, Kohonen-Corish M, Yip P, Yu B, O'Toole SA, McCaughan BC, *et al*: PD-L1 expression is a favorable prognostic factor in early stage non-small cell carcinoma. Lung Cancer 89: 181-188, 2015.